Geophysical Research Letters

Causality of an extreme harmful algal bloom in Monterey Bay, California, during the 2014–2016 northeast Pacific warm anomaly

J. P. Ryan[1], R. M. Kudela[2], J. M. Birch[1], M. Blum[1], H. A. Bowers[1,3], F. P. Chavez[1], G. J. Doucette[4], K. Hayashi[2], R. Marin III[1], C. M. Mikulski[4], J. T. Pennington[1], C. A. Scholin[1], G. J. Smith[3], A. Woods[3], and Y. Zhang[1]

[1]Research Division, Monterey Bay Aquarium Research Institute, Moss Landing, California, USA, [2]Ocean Sciences Department, University of California, Santa Cruz, California, USA, [3]Environmental Biotechnology Department, Moss Landing Marine Laboratories, Moss Landing, California, USA, [4]Marine Biotoxins Program, NOAA/National Ocean Service, Charleston, South Carolina, USA

Abstract An ecologically and economically disruptive harmful algal bloom (HAB) affected much of the northeast Pacific margin in 2015, during a prolonged oceanic warm anomaly. Caused by diatoms of the genus *Pseudo-nitzschia*, this HAB produced the highest particulate concentrations of the biotoxin domoic acid (DA) ever recorded in Monterey Bay, California. Bloom inception followed strong upwelling during the spring transition, which introduced nutrients and eliminated the warm anomaly locally. Subsequently, moderate and intermittent upwelling created favorable conditions for growth and accumulation of HAB biomass, which was dominated by a highly toxigenic species, *P. australis*. High cellular DA concentrations were associated with available nitrogen for DA synthesis coincident with silicate exhaustion. This nutrient influence resulted from two factors: (1) disproportionate depletion of silicate in upwelling source waters during the warm anomaly, the most severe depletion observed in 24 years, and (2) silicate uptake by the dense diatom bloom.

1. Introduction

During the 2014–2016 northeast Pacific warm anomaly [*Bond et al.,* 2015; *Di Lorenzo and Mantua*, 2016], an unprecedented harmful algal bloom (HAB) caused widespread ecological and economic impacts along the west coast of North America [*McCabe et al.,* 2016]. Harmful consequences resulted from food web transfer of the biotoxin domoic acid (DA), which is produced by several species in the diatom genus *Pseudo-nitzschia*. Upwelling systems, including the California Current System (CCS), are particularly prone to the detrimental consequences of DA outbreaks, which can cause illness and mortality in marine life and humans as well as economically disruptive fishery closures required to protect human health [*Scholin et al.,* 2000; *Kudela et al.,* 2005; *Trainer et al.,* 2012]. During the 2015 HAB, detection of DA in marine mammals—including whales, dolphins, porpoises, seals, and sea lions—spanned the largest geographic extent ever recorded [*McCabe et al.,* 2016]. Fishery closures prompted a congressional briefing and a request from the Governor of California for federal declaration of disaster and failure in commercial crab fisheries.

Observations in the northern CCS indicated that the warm anomaly allowed a highly toxigenic species, *P. australis*, to extend its range northward [*McCabe et al.,* 2016]. Nutrient provision by spring upwelling fueled the bloom, and transport of bloom biomass to the coast enabled trophic transfer of DA into razor clam and crab fisheries. In Monterey Bay, HAB development also coincided with spring upwelling. However, range expansion of *P. australis* was not a factor because this species is common to the central and southern CCS [*Scholin et al.,* 2000; *Schnetzer et al.,* 2007; *Trainer et al.,* 2012]. Further, spring upwelling eliminated warm anomalies in Monterey Bay during HAB inception and peak phases, indicating that temperature was not a primary physiological driver of the HAB and motivating consideration of nutrient influence on HAB toxicity. Of particular interest is the potential role of silicate limitation, which has been linked to increased toxicity in laboratory and field studies [*Bates et al.,* 1991; *Pan et al.,* 1996a, 1996b, 1998; *Fehling et al.,* 2004; *Anderson et al.,* 2006; *Schnetzer et al.,* 2007].

Development of the HAB in Monterey Bay was closely studied during a NOAA Ecology and Oceanography of Harmful Algal Blooms (ECOHAB) field program in spring 2015. Integrating intensive observations of this HAB with regional ecosystem observations from the last 24 years, we find that the extreme 2015 HAB in Monterey

Bay was caused by coincidence of strong upwelling at bloom inception, moderate and intermittent upwelling during bloom persistence, and anomalous background nutrient stoichiometry during the warm anomaly.

2. Materials and Methods

2.1. Regional Context: Physical Anomalies in the California Current System (CCS)

To examine physical anomalies in the CCS, we analyzed MEaSUREs multimission altimeter sea level anomaly (SLA) from NASA Jet Propulsion Laboratory, version 4.0 data between January 1993 and November 2016. Original 10 day data were temporally averaged to seasonal and spatially averaged for the CCS. The CCS domain was specified following *Auad et al.* [2011]: 23°N to 43°N within 800 km of the coast. Seasonal variations in CCS mean SLA were removed by subtracting the seasonal climatology from the seasonal mean time series.

2.2. Ecosystem Dynamics in Monterey Bay

Sampling locations for examining ecosystem variations in the Monterey Bay region are shown in Figure 1a. Surface hydrographic variations at the mouth of Monterey Bay during 2015 were examined using daily mean temperature and salinity data at mooring M1 (36.75°N, 122°W). To examine long-term variations at M1 in relation to the CCS (section 2.1), seasonal anomalies were computed for the period in which satellite SLA data were available, 1993–2016. Wind forcing was examined using hourly wind speed and direction data from NOAA station 46042 (36.791°N, 122.452°W). Daily mean alongshore wind speed was computed for 1993–2016. An annual climatology at daily resolution, computed from the 24 years of data, was used to evaluate the strength of wind forcing leading into inception of the 2015 HAB.

Phytoplankton and toxin data were derived from multiple sample sources (Figure 1a): Environmental Sample Processor (ESP) instruments moored in the mixed layer of the northern and southern bay, targeted sampling by an AUV, and weekly surface sampling at Santa Cruz Wharf (SCW). ESP methods for detection and quantification of *Pseudo-nitzschia* species and particulate DA [*Greenfield et al.,* 2008; *Doucette et al.,* 2009] and ESP applications to HAB research in Monterey Bay [*Ryan et al.,* 2011, 2014a] and the Southern California Bight [*Seegers et al.,* 2015] have been described. In this study, each ESP acquired and processed 21 samples between 11 May and 7 June 2015. Amid tidal variations the average ESP sample depths were 4 m (south) and 6 m (north). AUV sampling autonomously targeted phytoplankton bloom patches while conducting high-resolution surveys, as previously applied to plankton ecology research [*Zhang et al.,* 2010; *Ryan et al.,* 2014a, 2014b].

Enumeration of phytoplankton in AUV samples followed the methods used in weekly phytoplankton monitoring at Monterey Wharf [*Woods,* 2016]. Weekly sampling from Santa Cruz Wharf provided time series of toxigenic *Pseudo-nitzschia* and particulate DA (pDA) concentrations. Quantification of toxigenic *Pseudo-nitzschia* abundance used molecular detection targeting *P. australis*, *P. multiseries,* and *P. pseudodelicatissima* [*Miller and Scholin,* 1998]. Quantification of pDA was by enzyme-linked immunosorbent assay prior to 2009 and liquid chromatography-mass spectrometry thereafter [*Lane et al.,* 2010]. The reporting limit of detection for both methods was 3 ng L^{-1}, and they have been compared to ensure consistency across the time series [*Litaker et al.,* 2008; *Seubert et al.,* 2014]. To place 2015 cell and pDA concentrations in a longer-term perspective, we aggregated available Monterey Bay data that consistently quantified toxigenic *Pseudo-nitzschia* as the sum of molecular probe based concentrations of *P. australis* and *P. multiseries*. This included two data sources: (1) weekly sampling from Santa Cruz Wharf for 2007–2015 and (2) results from prior ESP deployments [*Ryan et al.,* 2011, 2014a].

More than two decades of nutrient monitoring in Monterey Bay provide a basis for examining anomalous chemical influences on the 2015 HAB. Since 1993 complete nutrient profiles at M1 (Figure 1a) were acquired on average every 28 days, providing a robust basis for examining seasonal means and their departures from climatology. Anomalies were computed from average concentrations in the upper 40 m; this spans the depth range over which HAB populations were observed during the 2015 ECOHAB study. Ship sampling and measurements followed published protocols [*Pennington and Chavez,* 2000], both throughout the time series and during sampling that augmented the 2015 ECOHAB study.

Satellite remote sensing data were used for regional context, specifically Visible Infrared Imaging Radiometer Suite chlorophyll and Advanced Very High Resolution Radiometer sea surface temperature (SST), both
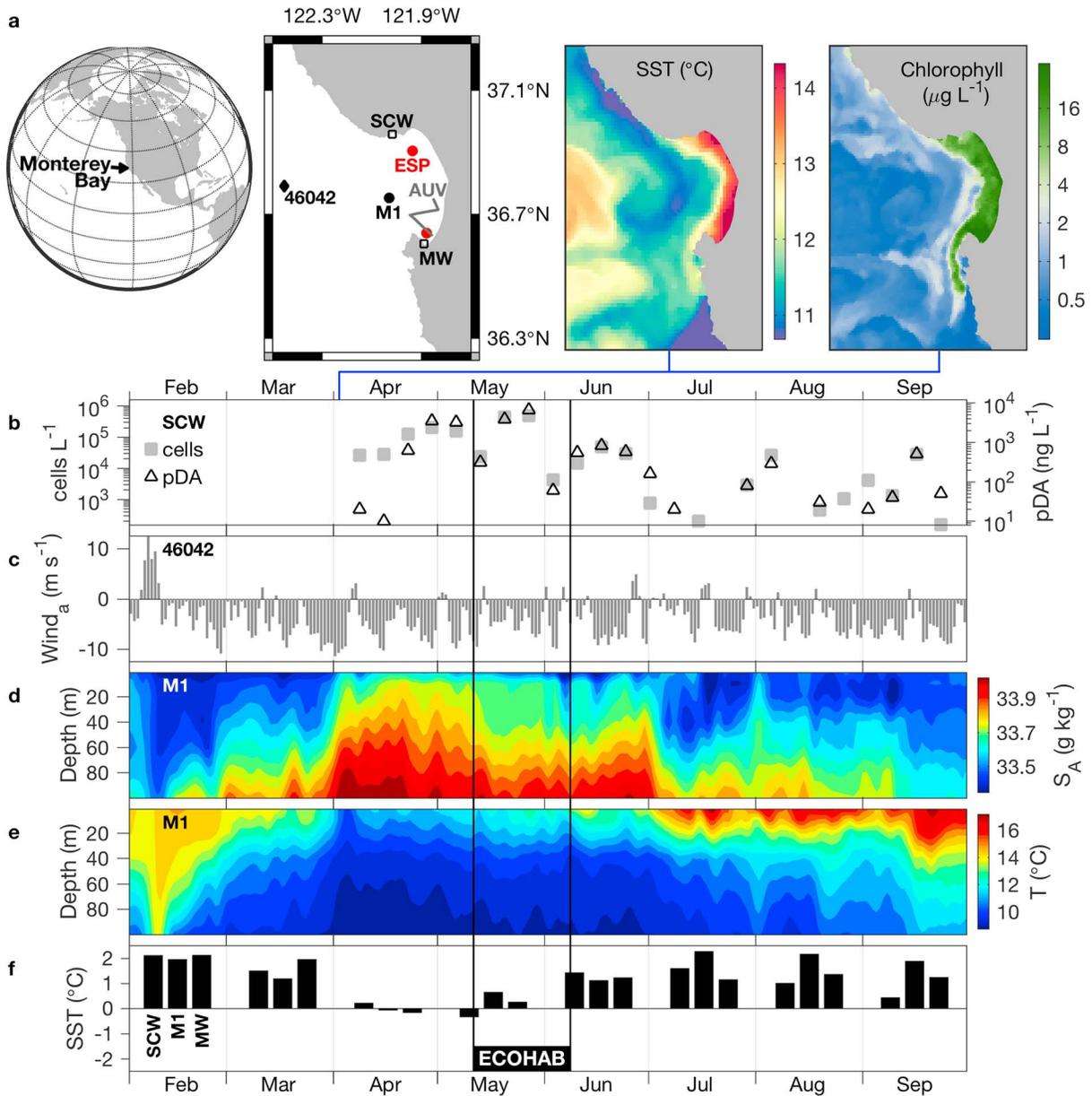
Figure 1. The 2015 HAB development in Monterey Bay, California. (a) Maps of observing locations (left) and regional conditions on 2 April 2015 (right). (b) Concentrations of toxigenic *Pseudo-nitzschia* and particulate DA at SCW. Weekly sampling occurred throughout the period shown; signals were below the limit of detection (100 cells per liter; 3 ng L^{-1} pDA) prior to April. (c) Daily mean alongshore wind speed at NOAA buoy 46042; negative values are upwelling favorable. (d, e) Daily mean salinity and temperature at mooring M1. (f) Monthly mean surface temperature anomalies at SCW, M1, and MW. The period of the ECOHAB field program is indicated.

acquired through the NOAA ERDDAP server (coastwatch.pfeg.noaa.gov/erddap/). Satellite data coverage was too sparse to support effective time series analysis; however, available observations provided relevant context during HAB inception.

3. Results and Discussion

3.1. HAB Inception and Development

In 2015 toxic *Pseudo-nitzschia* and pDA were first detected from weekly sampling at SCW on 8 April (Figures 1a and 1b), shortly following the strongest upwelling favorable winds of the spring transition

during late March through early April (Figure 1c). Between 24 March and 4 April, upwelling favorable winds averaged 4.5 m s^{-1} stronger than climatology. Outcropping of deep isohalines and isotherms at M1 during early April (Figures 1d and 1e) indicate the influx of upwelled waters that provided nutrients to fuel HAB inception. While warm anomalies prevailed at SCW, M1, and MW during February–March, the strong upwelling largely eliminated the warm anomaly during April–May (Figure 1f).

The process of nutrient supply from wind-driven upwelling to Monterey Bay is illustrated by SST patterns (Figure 1a). The SST image from 2 April 2015 shows a typical pattern of cold upwelled water originating north of Monterey Bay and flowing southward into the bay and into an eddy outside the bay [*Rosenfeld et al.,* 1994]. The biological response to nutrient supply is illustrated by surface chlorophyll patterns (Figure 1a). By 2 April a phytoplankton bloom was developing in the bay. The filaments of chlorophyll-rich water extending southward out of the southern bay indicate advection and entrainment of bloom populations in response to flow of upwelled water into the bay, yet most of the bloom was evidently retained within the bay.

Following the maximum cold/saline upwelling signal that persisted from early April to early May (Figures 1d and 1e), maxima in cell concentrations and pDA were observed during May while the ECOHAB field program was conducted (Figure 1b). Cycles of moderate upwelling and relaxation occurred during this peak bloom period (Figure 1c), alternating nutrient supply with calm periods allowing for phytoplankton growth and accumulation. Using satellite observations and numerical model simulations of the CCS, *Jacox et al.* [2016] show that optimal accumulation of phytoplankton biomass occurs under moderate wind stress, between nutrient limitation associated with lower wind stress and export processes (advection, mixing, and subduction) associated with higher wind stress.

HAB populations and favorable conditions for their growth and accumulation were observed in greater detail using an AUV (Figure 2). AUV surveys targeted the southern bay because real-time ESP results indicated higher concentrations of *P. australis* and pDA in the southern bay (locations of ESP moorings and AUV surveys in Figure 1a). Cell and toxin concentrations in bloom layers (Figures 2a and 2b) were higher than those observed at Santa Cruz Wharf (Figure 1b), with cell concentrations as high as 2.53×10^6 cells per liter and pDA concentrations as high as 31,700 ng L^{-1} in the densely concentrated layers. The bloom layers were completely dominated by *Pseudo-nitzschia*, largely the seriata size class (Figure 2a), which includes the most toxic species in this region: *P. australis* and *P. multiseries*. Molecular probe results for multiple *Pseudo-nitzschia* species showed that *P. australis* comprised 93% of the toxigenic *Pseudo-nitzschia* population on average in samples from the ESP moorings (*n* = 42).

The AUV surveyed the water column and sampled HAB populations during contrasting upwelling conditions. During a relaxation of upwelling, phytoplankton populations were concentrated in the thermocline/nutricline (Figure 2, left panels, 28 May). During subsequent intensification of upwelling, changes included water column cooling, nutrient enrichment, and shoaling of phytoplankton populations (Figure 2, right panels, 5 June). Ship-based sampling at the southern ESP location on these two days also showed changes in nutrient availability and primary productivity. On 28 May, nitrate and silicate were not detectable in the upper 10 m and maximum primary productivity in the water column was 57 mg C m^{-3} d^{-1}. On 5 June, average nitrate and silicate concentrations in the upper 10 m were 2.9 and 1.2 μM, respectively, and maximum primary productivity was 540 mg C m^{-3} d^{-1}.

These variations illustrate the basis for growth and accumulation of HAB biomass. When populations resided in the nutricline, the overlying water was clear (light transmission levels above the bloom layer at ESP South were ~87%), thereby maximizing light penetration to the subsurface HAB populations. Subsequent upwelling shoaled HAB populations, thereby increasing light exposure while supplying nutrients to the surface mixed layer. Biomass accumulation may have been influenced by settling of populations into the nutricline and by retention of populations within the bay through repeated responses to intermittent nutrient supply.

Concentrations of toxic *Pseudo-nitzschia* and pDA at SCW decreased from the April–May peak, in association with freshening and warming of the upper water column during June–July (Figures 1b, 1d, and 1e). These hydrographic and biological changes are consistent with the typical response to relaxation of upwelling favorable winds, involving influx of offshore low-salinity, low-chlorophyll water [e.g. *Ryan et al.,* 2011, 2014a]. Relaxation of upwelling wind forcing was particularly prevalent during late May to early June and late June to mid-July (Figure 1c), and warm anomalies returned to all three monitoring locations in the bay during
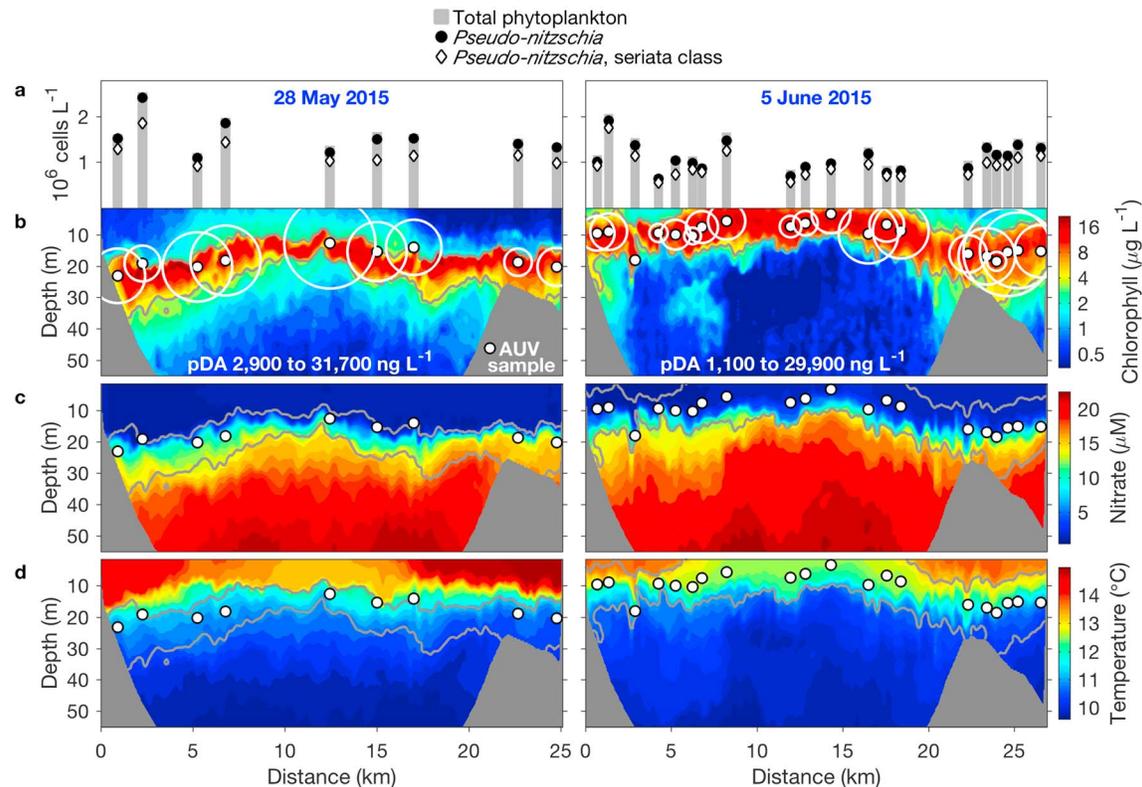
Figure 2. Environmental forcing of phytoplankton growth and accumulation. AUV mapping and targeted sampling of HAB layers were conducted during a relaxation response (28 May 2015, left) and an upwelling response (5 June 2015, right). The AUV transect location is shown in Figure 1a; surveys progressed south to north. (a) Cell counts from microscopy; results are shown directly above the sample locations (indicated by the solid white circles in Figures 2b–2d). (b–d) Chlorophyll concentration, nitrate concentration, and temperature along the AUV transect. The HAB layer is highlighted in each panel by gray contours. In the chlorophyll sections (Figure 2b), particulate DA concentrations are represented by the size of the open white circle around each sample location, and the range in each survey is noted.

June (Figure 1f). Weak HAB signals at SCW during July coincided with dramatic freshening and warming, and the remainder of the year was marked by relatively weak and intermittent HAB signals coincident with persistent warm, low salinity conditions (Figures 1b–1f). The SCW time series thus defines a primary HAB period of April–June, when high concentrations of cells and toxin persisted. Environmental conditions during this HAB period will next be examined from a long-term perspective.

3.2. A Biologically Exceptional HAB in a Chemically Exceptional Environment

Impacts of a toxic phytoplankton bloom are determined by the biomass of toxigenic cells, per-cell toxin production rates, toxin intracellular retention, and trophic transfer efficiency [*Trainer et al.,* 2012]. This study focuses on the bloom and does not examine trophic transfer of DA. Relative to measurements made since 2007 in Monterey Bay, during the 2015 HAB toxic *Pseudo-nitzschia* reached exceptionally high abundances, and intracellular DA concentrations reached high levels within these dense populations (Figures 3a and 3b).

Occurrence of this dense bloom can be explained by favorable conditions for growth and accumulation (section 3.1). Understanding the occurrence of high cellular toxicity requires consideration of physical and chemical conditions. Anomalous temperature would not have influenced toxicity because warm anomalies were eliminated during HAB inception and peak phases (Figure 1f, April–May). Consistent with local in situ data, regional remote sensing data show that SST anomalies were insignificant in the greater CCS surrounding Monterey Bay during April–May [*Gentemann et al.,* 2017]. However, nutrient anomalies did occur. Average nutrient profiles in the Monterey Bay region for April–June (1993–2016) show that silicate concentration normally exceeds nitrate concentration (Figure 3d). During April–June 2015 this average condition was reversed amid relatively low macronutrient concentrations (Figure 3e). All 24 profiles during
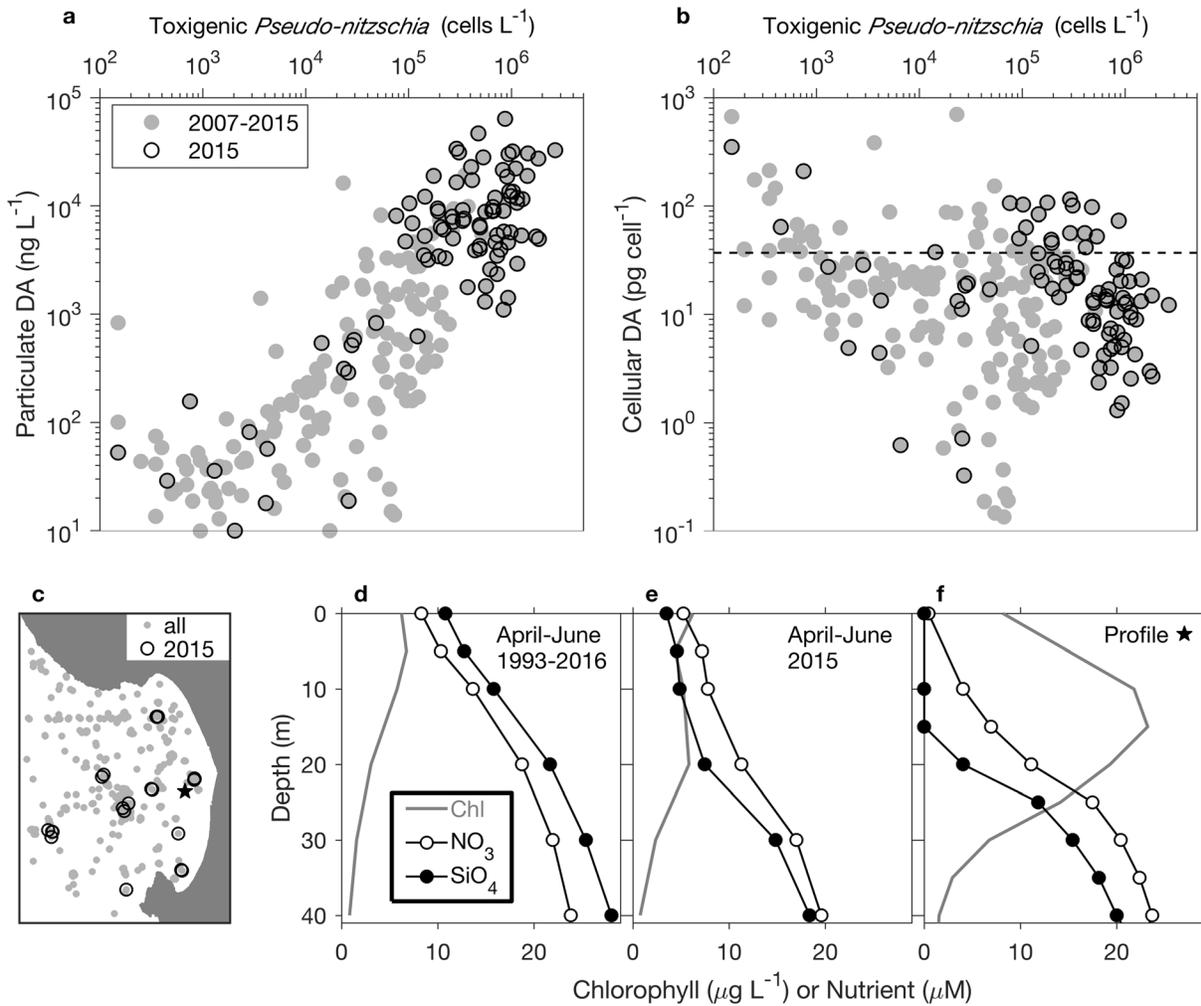
Figure 3. A biologically anomalous HAB in a chemically anomalous environment. Biological distinction of 2015 HAB populations is represented for (a) total particulate DA and (b) cellular DA. The dashed line in Figure 3b marks the highest reported concentration in cultured *P. australis* [*Trainer et al.,* 2012]. (c) Map shows the locations of all chlorophyll and nutrient measurements during April–June of 1990 through 2016 within and immediately adjacent to Monterey Bay. Locations of measurements during April–June 2015 (black circles) and an individual profile from 29 May 2015 (star) are distinguished. (d) Mean profiles of April–June chlorophyll and nutrient data from the full time series (2466 measurements in the upper 40 m). (e) Mean profiles of April–June data from 2015 (101 measurements in the upper 40 m). (f) Profiles through a dense HAB patch sampled on 29 May 2015 at the starred location in Figure 3c.

April–June 2015 showed this condition (locations in Figure 3c). In dense HAB populations (layers in Figure 2) silicate exhaustion occurred while nitrate remained available over approximately the upper half of the HAB layer (Figure 3f; above 15 m).

Disproportionate depletion of silicate may have been caused partly by the high silicate demand of the intense diatom bloom. Yet diatom blooms are typical of the spring upwelling period in this region, so this is unlikely to explain the anomalous chemical environment of the 2015 HAB (Figures 3d and 3e). The northeast Pacific warm anomaly peaked off California in 2015 [*Gentemann et al.,* 2017] and may have been associated with large-scale chemical consequences. This is examined using a 24 year time series from the mouth of Monterey Bay.

In this 24 year record the most exceptional positive anomalies in both Monterey Bay SST and CCS SLA are those of the 2014–2016 northeast Pacific warm anomaly, far exceeding those of the major 1997–1998 El Niño (Figure 4a). Throughout the time series low-frequency variation in SST at M1 generally tracks variation in sea level in the greater CCS (r^2 for annual means = 0.68). Salinity anomalies at M1 transitioned from positive to negative during the 2014–2016 warm anomaly (Figure 4b), a pattern observed
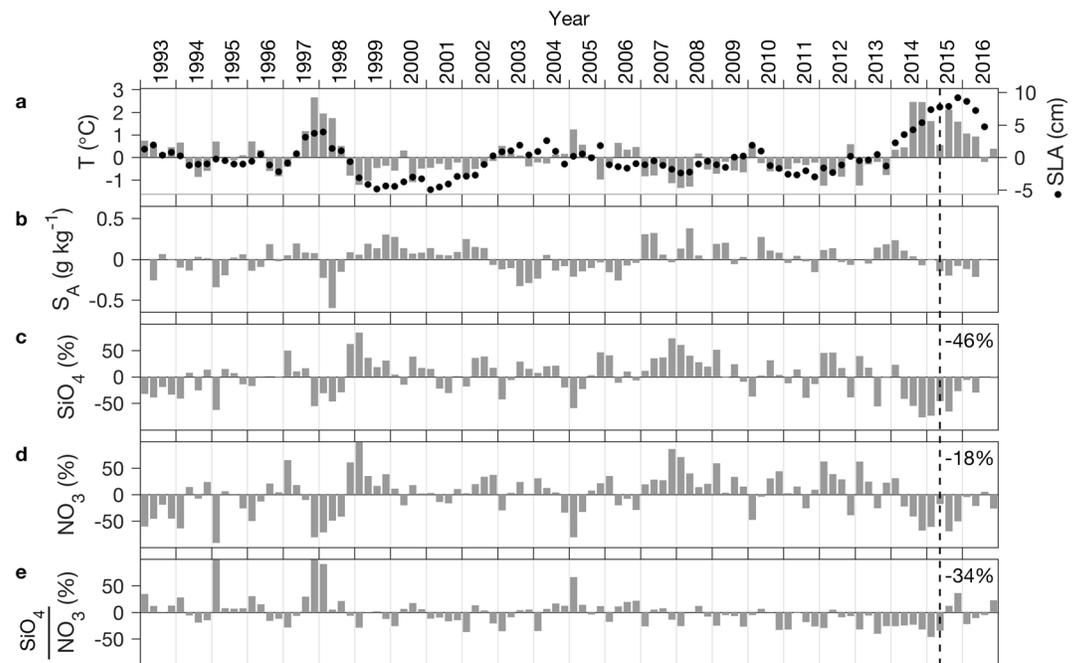
Figure 4. Long-term physical and chemical context for the 2015 HAB. Seasonal anomalies at the mouth of Monterey Bay from mooring and ship sampling time series (location M1 in Figure 1a): (a) surface temperature, (b) surface salinity, (c, d) average concentrations of silicate and nitrate in the upper 40 m, and (e) the ratio of silicate to nitrate, each averaged over 0–40 m. Nutrient anomalies (Figures 4c–4e) are normalized as percent differences relative to climatological seasonal means; percentages at the right of each panel are values for the April–June 2015 HAB period (marked by the vertical dashed line across all panels). The first positive anomaly in 1995 in Figure 4e is clipped as the range was constrained for visibility of the rest of the time series. Overlaid in Figure 4a is mean sea level anomaly (SLA) in the California Current System.

throughout the central and southern CCS [*Zaba and Rudnick*, 2016]. Concentrations of nitrate and silicate exhibited strong and persistent negative anomalies during 2014–2015 (Figures 4c and 4d). Negative nitrate anomalies of this magnitude were observed during the 1992–1993 and 1997–1998 El Niño events. In contrast, the negative silicate anomalies of 2014–2015 were by far the greatest in magnitude and duration of the entire record. There was thus disproportionate depletion of silicate relative to nitrate during 2014–2015. $SiO_4:NO_3$ ratios began exhibiting persistent negative anomalies in late 2013, and minimum ratios of the 24 year record occurred in the season immediately preceding the 2015 HAB (Figure 4e). This same pattern is evident in deeper water (40–80 m), indicating altered nutrient ratios in upwelling source waters. During the 2015 HAB (dashed line in Figure 4), upwelling increased nitrate and silicate concentrations. While nitrate concentrations returned to 18% below climatology with upwelling nutrient influx, silicate remained 46% below climatology. Phosphate concentrations were 10% below climatology during the 2015 HAB (not shown).

The nature of this chemical anomaly is consistent with enhancement of *Pseudo-nitzschia* toxicity. Laboratory studies have shown that silicate limitation can increase DA production in toxigenic *Pseudo-nitzschia* [*Bates et al.*, 1991; *Pan et al.*, 1996a, 1996b; *Fehling et al.*, 2004]. A nitrogen source is required for synthesis of DA; thus, N limitation restricts its synthesis [*Pan et al.*, 1998]. In contrast, Si or P limitation in the presence of sufficient N reduces primary metabolic activity and may promote the secondary metabolism of DA synthesis [*Pan et al.*, 1998; *Terseleer et al.*, 2013]. Further, cellular DA concentrations depend on interaction between the rates of DA production and cell division [*Trainer et al.*, 2012]. During early senescence, dilution of cellular DA via cell division slows, and cellular DA increases if the production rate of DA is maintained. During March–June 2015, intense upwelling followed by moderate intermittent upwelling enabled establishment of dense HAB populations within Monterey Bay. We speculate that the moderate and intermittent upwelling that followed HAB initiation repeatedly returned bloom populations to early senescence as nutrients were depleted between upwelling events. The anomalously low silicate:nitrate ratios would cause silicate to be exhausted before nitrate (Figure 3f), thus promoting populations with high cellular DA, as observed (Figures 2b, 3a, and 3b).

Other field data have yielded mixed results on the relationships between *Pseudo-nitzschia* toxicity and nutrient concentrations or ratios. *Trainer et al.* [2000] found no evidence for the role of the SiO_4:NO_3 ratio in CCS data. In contrast, *Anderson et al.* [2006] found maximal toxin production associated with low SiO_4:NO_3 ratios in a bloom in the Santa Barbara Channel, and *Schnetzer et al.* [2007] found an inverse correlation between concentrations of silicic acid and pDA in data from the Southern California Bight. The multidecadal perspective of the present study reveals that highly anomalous nutrient stoichiometry coincided with the 2014–2016 warm anomaly. The nature of this chemical anomaly is consistent with causality of high cellular DA within the dense bloom that developed in Monterey Bay. Over the 24 year record, the SiO_4:NO_3 anomaly reached its lowest level immediately before the spring transition that initiated the HAB. Macronutrient anomalies have since been negative or near zero (Figures 4c and 4d), and the SiO_4:NO_3 anomaly has varied between positive and negative (Figure 4e). The warm anomaly persisted into 2016 [*Gentemann et al.,* 2017], and continuing nutrient monitoring will reveal the evolution of nutrient stoichiometry and its potential influence on toxigenic *Pseudo-nitzschia* blooms.

4. Conclusions

Consistent with the severe ecosystem and economic repercussions of the 2015 northeast Pacific DA outbreak, HAB indicators in Monterey Bay clearly defined a biologically anomalous event marked by concurrence of high cell and toxin concentrations. As in the northern CCS [*McCabe et al.,* 2016], the Monterey Bay bloom was dominated by a highly toxigenic species, *P. australis*, and its initiation coincided with the spring upwelling transition. Because temperature in Monterey Bay was near normal during HAB inception and peak phases, temperature was probably not a primary physiological influence. In contrast, anomalous nutrient stoichiometry likely increased cellular toxicity. This association may be examined elsewhere in the CCS, where nutrient time series data are sufficient. Further, other low-frequency variations are important to consider. For example, trends in the southern CCS for 1984–2012 include decreasing Si:N ratios in the depth range of upwelling source water, a pattern attributed to low-frequency variation in source water masses [*Bograd et al.,* 2015]. This nutrient anomaly in the CCS may prove increasingly important in determining the nature and consequences of toxic diatom blooms in a changing ocean. Inclusion of silicate in observational and modeling approaches [e.g., *Anderson et al.,* 2009; *Terseleer et al.,* 2013] will be important to advancing prediction of *Pseudo-nitzschia* HABs and their associated toxicity.

References

Anderson, C. R., M. A. Brzezinski, L. Washburn, and R. Kudela (2006), Circulation and environmental conditions during a toxigenic *Pseudo-nitzschia australis* bloom in the Santa Barbara Channel, California, *Mar. Ecol. Prog. Ser., 327*, 119–133.

Anderson, C. R., D. A. Siegel, R. M. Kudela, and M. A. Brezinski (2009), Empirical habitat models of toxigenic *Pseudo-nitzschia* spp.: Potential use as a remote detection tool in the Santa Barbara Channel, *Harmful Algae, 8*, 478–492, doi:10.1016/j.hal.2008.10.005.

Auad, G., D. Roemmich, and J. Gilson (2011), The California Current System in relation to the Northeast Pacific Ocean circulation, *Prog. Oceanogr., 91*, 576–592.

Bates, S. S., A. S. W. de Freitas, J. E. Milley, R. Pocklington, M. A. Quilliam, J. C. Smith, and J. Worms (1991), Controls on domoic acid production by the diatom *Nitzschia pungens* f. multiseries in culture: Nutrients and irradiance, *Can. J. Fish. Aquat. Sci., 48*, 1136–1144.

Bograd, S. J., M. Pozo Buil, E. Di Lorenzo, C. G. Castro, I. D. Schroeder, R. Goericke, C. R. Anderson, C. Benitez-Nelson, and F. A. Whitney (2015), Changes in source waters to the Southern California Bight, *Deep Sea Res., Part II, 112*, 42–52, doi:10.1016/j.dsr2.2014.04.009.

Bond, N. A., M. F. Cronin, H. Freeland, and N. Mantua (2015), Causes and impacts of the 2014 warm anomaly in the northeast Pacific, *Geophys. Res. Lett., 42*, 3414–3420, doi:10.1002/2015GL063306.

Di Lorenzo, E., and N. Mantua (2016), Multi-year persistence of the 2014/15 North Pacific marine heatwave, *Nat. Clim. Change, 6*, 1042–1047, doi:10.1038/nclimate3082.

Doucette, G. J., C. M. Mikulski, K. L. Jones, K. L. King, D. I. Greenfield, R. Marin III, S. Jensen, C. T. Elliott, and C. A. Scholin (2009), Remote, subsurface detection of the algal toxin domoic acid onboard the environmental sample processor: Assay development and field trials, *Harmful Algae, 8*, 880–888.

Fehling, J., K. Davidson, C. J. Bolch, and S. S. Bates (2004), Growth and domoic acid production by *Pseudo-nitzschia seriata* (Bacillariophyceae) under phosphate and silicate limitation, *J. Phycol., 40*, 674–683, doi:10.1111/j.1529-8817.2004.03213.x.

Gentemann, C. L., M. R. Fewings, and M. García-Reyes (2017), Satellite sea surface temperatures along the West Coast of the United States during the 2014–2016 northeast Pacific marine heat wave, *Geophys. Res. Lett., 44*, 312–319, doi:10.1002/2016GL071039.

Greenfield, D. I., R. Marin III, G. J. Doucette, C. M. Mikulski, K. L. Jones, S. Jensen, B. Roman, N. Alvarado, J. Feldman, and C. A. Scholin (2008), Field applications of the second-generation environmental sample processor (ESP) for remote detection of harmful algae: 2006–2007, *Limnol. Oceanogr. Methods, 6*, 667–679.

Jacox, M. G., E. L. Hazen, and S. J. Bograd (2016), Optimal environmental conditions and anomalous ecosystem responses: Constraining bottom-up controls of phytoplankton biomass in the California Current System, *Sci. Rep., 6*, 27,612, doi:10.1038/srep27612.

Kudela, R., G. Pitcher, T. Probyn, F. Figueiras, T. Moita, and V. Trainer (2005), Harmful algal blooms in coastal upwelling systems, *Oceanography, 18*, 184–197.

Lane, J. Q., C. M. Roddam, G. W. Langlois, and R. M. Kudela (2010), Application of Solid Phase Adsorption Toxin Tracking (SPATT) for field detection of the hydrophilic phycotoxins domoic acid and saxitoxin in coastal California, *Limnol. Oceanogr. Methods*, *8*, 645–660.

Litaker, R. W., et al. (2008), Rapid enzyme-linked immunosorbent assay for detection of the algal toxin domoic acid, *J. Shellfish. Res.*, *27*, 1301–1310.

McCabe, R. M., B. M. Hickey, R. M. Kudela, K. A. Lefebvre, N. G. Adams, B. D. Bill, F. M. D. Gulland, R. E. Thomson, W. P. Cochlan, and V. L. Trainer (2016), An unprecedented coastwide toxic algal bloom linked to anomalous ocean conditions, *Geophys. Res. Lett.*, *43*, 10,366–10,376, doi:10.1002/2016GL070023.

Miller, P. E., and C. A. Scholin (1998), Identification and enumeration of cultured and wild *Pseudo-nitzschia* (Bacillariophyceae) using species-specific LSU rRNA-targeted fluorescent probes and filter-based whole cell hypridization, *J. Phycol.*, *34*, 371–382.

Pan, Y. L., D. V. Subba Rao, K. H. Mann, R. G. Brown, and R. Pocklington (1996a), Effects of silicate limitation on production of domoic acid, a neurotoxin, by the diatom *Pseudo-nitzschia multiseries*: 1. Batch culture studies, *Mar. Ecol. Prog. Ser.*, *131*, 225–233.

Pan, Y. L., D. V. Subba Rao, K. H. Mann, W. K. W. Li, and W. G. Harrison (1996b), Effects of silicate limitation on production of domoic acid, a neurotoxin, by the diatom *Pseudo-nitzschia multiseries*: 2. Continuous culture studies, *Mar. Ecol. Prog. Ser.*, *131*, 235–243.

Pan, Y., S. S. Bates, and A. D. Cembella (1998), Environmental stress and domoic acid production by *Pseudo-nitzschia*: A physiological perspective, *Nat. Toxins*, *6*, 127–135.

Pennington, J. T., and F. P. Chavez (2000), Seasonal fluctuations of temperature, salinity, nitrate, chlorophyll and primary production at station H3/M1 over 1989–1996 in Monterey Bay, California, *Deep Sea Res., Part II*, *47*, 947–973, doi:10.1016/S0967-0645(99)00132-0.

Rosenfeld, L. K., F. B. Schwing, N. Garfield, and D. E. Tracy (1994), Bifurcated flow from an upwelling center: A cold water source for Monterey Bay, *Cont. Shelf Res.*, *14*, 931–964.

Ryan, J., et al. (2011), Harmful phytoplankton ecology studies using an autonomous molecular analytical and ocean observing network, *Limnol. Oceanogr.*, *56*, 1255–1272, doi:10.4319/lo.2011.56.4.1255.

Ryan, J. P., et al. (2014a), Boundary influences on HAB phytoplankton ecology in a stratification-enhanced upwelling shadow, *Deep Sea Res., Part II*, *101*, 63–79, doi:10.1016/j.dsr2.2013.01.017.

Ryan, J. P., J. B. J. Harvey, Y. Zhang, and B. Woodson (2014b), Distributions of invertebrate larvae and phytoplankton in a coastal upwelling system retention zone and peripheral front, *J. Exp. Mar. Biol. Ecol.*, *459*, 51–60, doi:10.1016/j.jembe.2014.05.017.

Schnetzer, A., P. E. Miller, R. A. Schaffner, B. A. Stauffer, B. H. Jones, S. B. Weisberg, P. M. DiGiacomo, W. M. Berelson, and D. A. Caron (2007), Blooms of *Pseudo-nitzschia* and domoic acid in the San Pedro Channel and Los Angeles harbor areas of the Southern California Bight, 2003–2004, *Harmful Algae*, *6*, 372–387, doi:10.1016/j.hal.2006.11.004.

Scholin, C. A., et al. (2000), Mortality of sea lions along the central California coast linked to a toxic diatom bloom, *Nature*, *403*, 80–84.

Seegers, B. N., J. M. Birch, R. Marin III, C. A. Scholin, D. A. Caron, E. L. Seubert, M. D. A. Howard, G. L. Robertson, and B. H. Jones (2015), Subsurface seeding of surface harmful algal blooms observed through the integration of autonomous gliders, moored environmental sample processors, and satellite remote sensing in southern California, *Limnol. Oceanogr.*, *60*, 754–764, doi:10.1002/lno.10082.

Seubert, E. L., M. D. A. Howard, R. M. Kudela, T. N. Stewart, R. W. Litaker, R. Evans, and D. A. Caron (2014), Development, comparison, and validation using ELISAs for the determination of domoic acid in California sea lion body fluids, *J. AOAC Int.*, *97*, 1–12, doi:10.5740/jaoacint. SGESeubert.

Terseleer, N. A., N. Gypens, and C. Lancelot (2013), Factors controlling the production of domoic acid by *Pseudo-nitzschia* (Bacillariophyceae): A model study, *Harmful Algae*, *24*, 45–53, doi:10.1016/j.hal.2013.01.004.

Trainer, V. L., N. G. Adams, B. D. Bill, C. M. Stehr, J. C. Wekell, P. Moeller, M. Busman, and D. Woodruff (2000), Domoic acid production near California coastal upwelling zones, June 1998, *Limnol. Oceanogr.*, *45*, 1818–1833.

Trainer, V. L., S. S. Bates, N. Lundholm, A. E. Thessen, N. G. Adams, W. P. Cochlan, and C. G. Trick (2012), *Pseudo-nitzschia* physiological ecology, phylogeny, toxicity, monitoring and impacts on ecosystem health, *Hamful Algae*, *14*, 271–300.

Woods, A. (2016), Monterey Wharf II weekly phytoplankton monitoring sample collection and processing notes, doi:10.17504/protocols.io. f2pbqdn.

Zaba, K. D., and D. L. Rudnick (2016), The 2014–2015 warming anomaly in the Southern California Current System observed by underwater gliders, *Geophys. Res. Lett.*, *43*, 1241–1248, doi:10.1002/2015GL067550.

Zhang, Y., R. S. McEwen, J. P. Ryan, and J. G. Bellingham (2010), Design and tests of an adaptive triggering method for capturing peak samples in a thin phytoplankton layer by an autonomous underwater vehicle, *IEEE J. Oceanic Eng.*, *35*, 785–796, doi:10.1109/JOE.2010.2081031.